ITS_LIVE Regional Glacier and Ice Sheet Surface Velocities

Last Update

June 19, 2019

Data Description

The Inter-Mission Time Series of Land Ice Velocity and Elevation (ITS_LIVE) project, part of NASA's Making Earth System Data Records for Use in Research Environments (MEaSUREs) 2017 program, provides global low-latency measurements of glacier and ice sheet surface velocity and elevation change at a high temporal resolution.

The ITS_LIVE data product presented here is a set of regional compilations of annual mean surface velocities for major glacier-covered regions, spanning the time period from 1985 to 2018, subject to image availability and quality. Surface velocities are derived from Landsat 4, 5, 7, and 8 imagery using the auto-RIFT feature tacking processing chain described in Gardner et al. (2018). Data scarcity and/or low radiometric quality are significant limiting factors for many regions in the earlier product years. Annual coverage is nearly complete for the years following the Landsat 8 launch in 2013.

Parameters

The parameters provided in this data set are listed in Table 1.

Table 1. List of Parameters

Parameter name	Description	Units	Class
`x`	Map-projected x-coordinate	m	double
`y`	Map-projected y-coordinate	m	double
`vx`	Velocity component in x-direction	m yr^{-1}	float
`vy`	Velocity component in y-direction	m yr^{-1}	float
`v`	Velocity magnitude	m yr^{-1}	float
`vx_err`	Error in `vx`	m yr^{-1}	float
`vy_err`	Error in `vy`	m yr^{-1}	float
`v_err`	Error in `v`	m yr^{-1}	float
`date`	Effective date	days since 01 January 0000*	float
`dt`	Effective image-pair date separation	days	uint
`count`	Number of velocities used in weighted average	count	uint
`chip_size_max`	Maximum accepted search chip size	m	uint
`ocean`	Ocean mask	binary	ushort
`rock`	Rock mask	binary	ushort
`ice`	Ice mask	binary	ushort

*The date is a serial date number that represents the whole number of days from a fixed, preset date (January 0, 0000) in the proleptic ISO calendar. January 1, 2000 = 730486 days from January 0, 0000.

File Information

Format

The data are provided as netCDF-4 HDF5 (`.nc`) files with embedded metadata. As a courtesy incomplete (no metadata) versions of the data are also provided as GeoTIFF, urls to virtual raster files (.vrt), and QGIS files that link to the .vrt files and contain regional base maps.

File Contents

Each netCDF file contains all of the parameters listed in Table 1, gridded at 240 m or 120 m over the regional map areas. Figure 1 shows an example of Antarctic velocity data (parameter `v` from Table 1) for three different years at 240 m resolution.

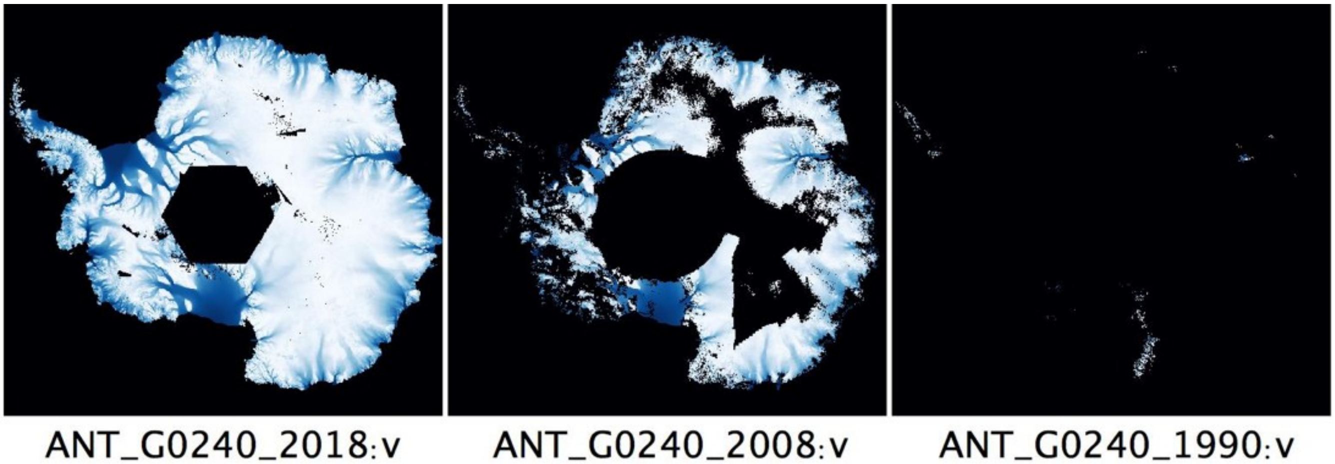

Figure 1. Example of Antarctic velocity data (v) at 240 m resolution for the years 2018, 2008, and 1990 (panels left to right).

Directory Structure

The files are organized into eight directories representing the eight mapped glacierized regions (see Figure 2 and Table 3): ALA (Alaska and Western North America), ANT (Antarctica), CAN (Arctic Canada), GRE (Greenland), HMA (High Mountain Asia), ICE (Iceland), PAT (Patagonian icefields), SRA (Svalbard and the Russian Arctic). The files are annual mappings of ice flow velocities from 1985 to 2018 (up to 34 annual mappings).

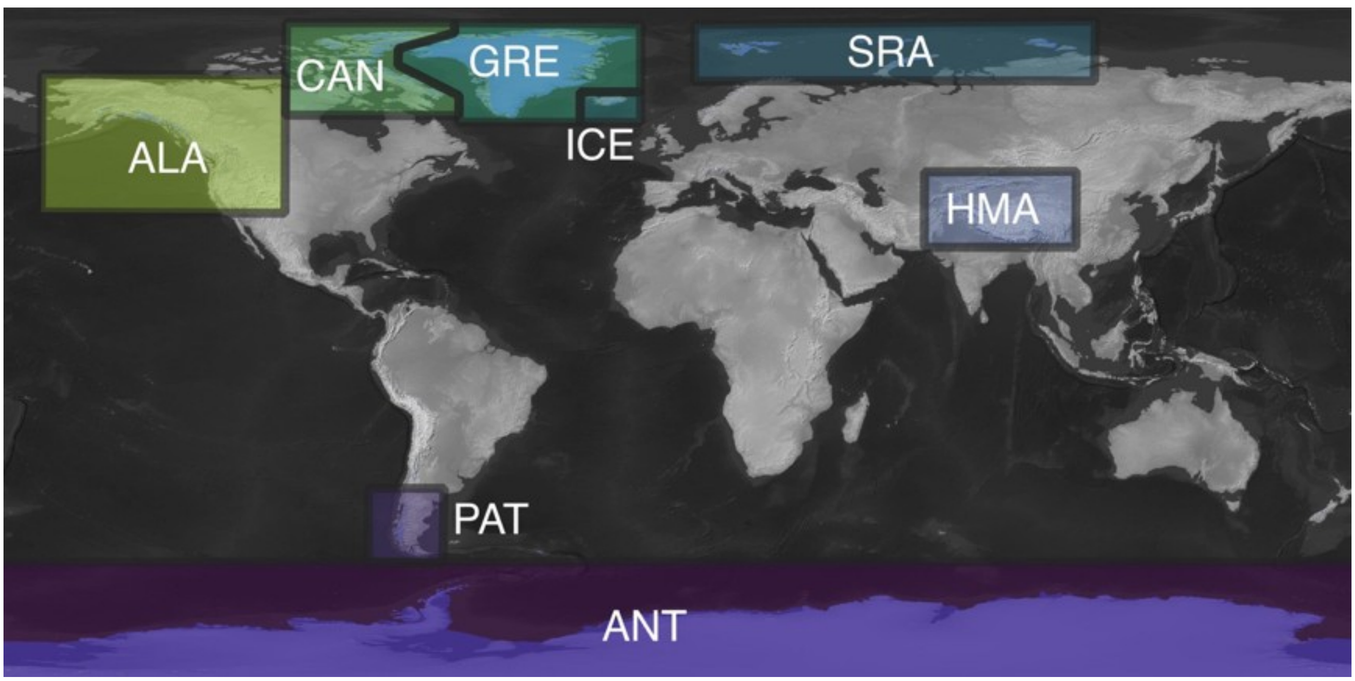

Figure 2. Geographic locations of the eight mapped glacierized regions (see Table 3).

Naming Convention

The file names include the region ID, as well as the survey year. Example file names:

```
ALA_G0240_2018.nc
ANT_G0120_0000.nc
```

The files are named according to the following convention, which is described in detail in Table 2:

```
regID_GXXXX_YYYY.ext
```

Table 2. File Naming Convention

Variable	Description
`regID`	Region ID (see Figure 2 and Table 3)
`GXXXX`	Grid (`G`) resolution in m. Values are either G0240 or G0120. Only time-averaged velocity (`YYYY` = 0000) is offered at 120 m resolution.
`YYYY`	Four-digit year of survey. Spans the years 1985 through 2018. The value of 0000 is the time-averaged or static velocity (i.e., error-weighted average of all years of data).
`.ext`	File type: netCDF (`.nc`) data file

File Size

The total file volume is approximately 104 GB. Individual NetCDF files range between 5 MB and 15 GB.

Spatial Information

Coverage

Spatial coverage varies in this data set and includes the eight regions listed in Table 3.

Resolution

240 m x 240 m
120 m x 120 m*

*cubic spline interpolation of underlying 240 m data and only for time-averaged velocity mosaic

Geolocation

Table 3 lists the eight different regions covered by the velocity mosaics and provides geolocation details for each region (see Figure 2).

Table 3. Region and Geolocation Information

Region ID	Name	Spatial resolution[1]	File sizes	EPSG code	Grid x min.	Grid x max.	Grid y min.	Grid y max.
ALA	Alaska and Western North America	240 m	~270 MB	3413	-4632847.5	-2791807.5	-1443712.5	1269007.5
ANT	Antarctica and periphery	240 m	~200 MB to 15 GB	3031	-2678287.5	2816512.5	-2154112.5	2259727.5
CAN	Arctic Canada South and North	240 m	~150 MB	3413	-1238287.5	-259327.5	-2881792.5	-585712.5
GRE	Greenland and periphery	240 m	~300 MB to 900 MB	3413	-645007.5	858112.5	-3369472.5	-641392.5
HMA	High Mountain Asia	240 m	~400 MB	102027	-2159887.5	652672.5	-264832.5	1643407.5
ICE	Iceland	240 m	~15 MB	3413	981232.5	1416832.5	-2630272.5	-2304112.5
PAT	Patagonian icefields	240 m	~5 MB to 50 MB	32718	537712.5	909952.5	3859327.5	4930447.5
SRA	Svalbard and Russian Arctic	240 m	~40 MB to 90 MB	3413	591472.5	1850752.5	-712192.5	1092367.5

[1]Spatial resolution for the time-averaged velocity grid is provided at 120 m and 240 m for all regions. File size for this file is four times greater than the largest value.

Temporal Information

Coverage

1985 to 2018

Resolution

Yearly*

*error weight average of all image-pair results with center dates that falls within that calendar year. The *date* field provides the error weighted average center date for each pixel and the *dt* field provides the error weighted average time separation between image pairs. Pixels with large *dt* (>300) can be considered average annual values while pixels with small *dt* (<180) can be considered average summer values.

Data Acquisition and Processing

Processing Steps

Image Preprocessing

All images are preprocessed using a 5x5 Wallis operator to normalize for local variability in image radiance caused by shadows, topography, and sun angle, all of which can generate spurious artifacts when applying feature tracking to derive surface flow from optical imagery. For Landsat 4 and 5 Band 2 images, along-track artifacts that are introduced from the Thematic Mapper whisk broom sensor are removed using Fourier filtering. Missing data in Landsat 7 images, introduced after the Scan Line Corrector failure (SLC-off), are filled with random noise so that they do not contribute to the amplitude of the correlation peak used in the feature tracking.

Image-pair velocities (auto-RIFT v1)

All image pairs are processed using the JPL autonomous Repeat Image Feature Tracking algorithms (auto-RIFT), first presented in (Gardner et al., 2018). Release v00.0 of the ITS_LIVE velocity mosaics use auto-RIFT Version 1. This ITS_LIVE data set uses surface displacements generated by image pairs in repeat orbits, and image pairs generated by overlap areas of adjacent or near-adjacent orbits. Image pairs collected from the same satellite position ("same-path-row") are searched if they have a time separation of fewer than 546 days. This approach was used for all satellites in the Landsat series (L4 to L8). To increase data density prior to the launch of Landsat 8, images acquired from differing satellite positions, generally in adjacent or near-adjacent orbit swaths ("cross-path-row"), are also processed if they have a time separation between 10 and 96 days and an acquisition date prior to 14 June 2013 (beginning of regular Landsat 8 data). Feature tracking of cross-path-row image pairs produces velocity fields with a lower signal-to-noise ratio due to residual parallax from imperfect terrain correction. Same-path-row and cross-path-row preprocessed pairs of images are searched for matching features by finding local normalized cross-correlation (NCC) maxima at sub-pixel resolution by oversampling the correlation surface by a factor of 16 using a Gaussian kernel. A sparse grid pixel-integer NCC search (1/16 of the density of full search grid) is used to determine areas of coherent correlation between image pairs. For more information, see the Normalized Displacement Coherence (NDC) filter described in Gardner et al. (2018). Results from the sparse search guide a dense search with search centers spaced such that there is no overlap between adjacent template windows. Areas of unsuccessful retrievals, as determined using the NDC filter, are searched with progressively increasing template chip sizes. Minimum and maximum acceptable template chip sizes for each search center are defined geographically and depend on land surface type (ice or rock), spatial gradient of a reference velocity, distance from ocean, and distance from ice edge.

To reduce computational demand, auto-RIFT employs a downstream search that centers the NCC search template window in the search image at the downstream location of the expected displacement between the two image pairs as determined from the reference velocity. The NCC search radius is unique in both x- and y-directions and varies spatially. The NCC search radius is defined according to the surface type (ice or rock), magnitude of the component reference velocity (vx, vy), and the distance from the ocean. Ocean area is identified according to the Global Self-consistent, Hierarchical, High-resolution Geography Database. In Greenland, land ice area is identified according to a data set provided by F. Paul (Bolch et al., 2013); in Antarctica land ice is identified according to Depoorter et al. (2013); everywhere else land ice is determined using the Randolf Glacier Index release 3.2. Rock is defined as neither ocean nor land ice. https://www.soest.hawaii.edu/pwessel/gshhg/

Quality, Errors, and Limitations

Image geometry between same-path-row image pairs is highly stable, but images suffer from x- and y-coordinate geolocation errors of 15 m. If uncorrected, a geolocation error of ~21 m, i.e. $(15^2 + 15^2)^{1/2}$, between two images separated in time by 16 days would introduce a bias in velocity of as much as ~480 m yr^{-1}. To correct for these errors, the component velocities `vx` and `vy` are tied to a "stable" surface wherein the median of each velocity component is set to zero over rock surfaces and set to the median reference velocity over slow-moving areas of Greenland and Antarctica (ice movement of less than 15 m yr^{-1}). For Greenland, the *MEaSUREs Greenland Annual Ice Sheet Velocity Mosaics from SAR and Landsat, Version 1* data are used as the reference velocity (Joughin et al., 2010); for Antarctica, the *MEaSUREs InSAR-Based Antarctica Ice Velocity Map, Version 2* data are used (Mouginot et al., 2012; Rignot et al., 2011).

The uncertainty of each image-pair velocity field is set equal to the standard error in component velocities relative to the stable surface velocity after applying the geolocation offset correction, if available. If an image-pair velocity field does not intersect a stable surface, the errors in `vx` and `vy` (parameters `vx_err` and `vy_err` in Table 1) are set to the RSS of the pointing uncertainty of both images. This error is updated to the standard deviation of the difference between the image-pair component velocities and the annual mean component velocities if the image-pair velocity is successfully co-registered during the creation of the annual mosaic that is described in the next section.

Velocities are calculated from imagery that has been map projected. This can introduce scale errors of up to a few percent that are dependent on the projection used and the location of the imagery. This distortion is corrected such that ITS_LIVE velocities represent horizontal velocities that would be measured by an observer on the ground. This has several implications:

1. When using ITS_LIVE velocities to calculate glacier flux, the flux gate cross-section needs to be corrected for projection scale distortion; however, ITS_LIVE velocities do not need to be corrected.
2. When calculating Lagrangian paths in map coordinates, the ITS_LIVE velocities should be scaled from velocities in ground units to velocities in map units to produce the appropriate speed in map coordinates.

Annual Mosaics (auto-RIFT v1)

Image-pair velocity fields can be contaminated by match blunders, such as matching along shadow edges or of surfaces obscured by clouds in one of the two images. Component velocities that deviate by more than three times the interquartile range from the median of all co-located pixels are assumed to be gross outliers and are removed. For normally distributed data, this approximates a 5-sigma filter.

Annual velocity maps are created by taking the error-weighted average of all image-pair velocity fields having a center-date that falls within that calendar year. The weight of each image-pair velocity field is calculated as:

$$w_{x/y,i} = \frac{1}{\sigma_{x/y,i}{}^2}$$

x/y denotes the velocity component, *i* the image pair velocity, and the error determined for each image-pair velocity. This is done iteratively to co-register image pair velocities that do not intersect the "stable" reference surface, and therefore do not have geolocation offset corrections. In the iterative process, all image-pair velocities with geolocation offset corrections are combined to create an annual velocity field that is then used to co-register image pair velocities that are lacking geolocation offset corrections. This later co-registration ties unregistered pairs to the annual velocity field where the error in the annual velocity field is less than 50 m yr^{-1}. This secondary co-registration is typically only evoked for large Antarctic ice shelves where the distances to exposed rock and/or slow-moving ice (less than 15 m yr^{-1}) can be large.

The error of the final annual mosaic is taken as:

$$\sigma_{x/y} = \sqrt{\frac{1}{\sum 1/\sigma^2_{x/y,i}}} = \sqrt{\frac{1}{\sum w_{x/y,i}}}$$

This approach, while allowing for the formal propagation of errors, typically produces errors that are unrealistically low. We suggest that the provided errors (parameters `vx_err`, `vy_err`, and `v_err` in Table 1), along with image-pair count (parameter `count` in Table 1), should be used as qualitative metrics for assessing errors. Annual mosaics are also provided with an effective date and image-pair time separation that are estimated for each pixel as a weighted average of the individual pairs' date and time span. A best estimate of the mean, or static, flow field for each region is provided by taking the weighted average of all years of data.

Instrumentation

The imagery used to create the velocity mosaics in this data set comes from the following sources:

- USGS/NASA's Landsat 4 (1982 to 1993) Thematic Mapper - Band 2 (30 m)
- USGS/NASA's Landsat 5 (1984 to 2013) Thematic Mapper - Band 2 (30 m)
- USGS/NASA's Landsat 7 (1999 to present) Enhanced Thematic Mapper Plus - Band 8 (15 m)
- USGS/NASA's Landsat 8 (2013 to present) Operational Land Imager - Band 8 (15 m)

All images with 60% cloud cover or less, as indicated in the image metadata, were processed. Landsat imagery was provided courtesy of the USGS and downloaded from Google Cloud (https://cloud.google.com/storage/docs/public-datasets/landsat).

Software and Tools

The netCDF files can be opened using geospatial software such as QGIS or Panoply. The metadata fields can be extracted using the gdalinfo command line utility available from the Geospatial Data Abstraction Library (GDAL) website.

Related Data Sets

Global Land Ice Velocity Extraction from Landsat 8 (GoLIVE), Version 1 (NSIDC-0710)

Landsat 8 Ice Speed of Antarctica (LISA), Version 1 (NSIDC-0733)

MEaSUREs Greenland Ice Velocity: Selected Glacier Site Velocity Maps from InSAR, Version 1 (NSIDC-0481)

MEaSUREs Annual Antarctic Ice Velocity Maps 2005-2017, Version 1 (NSIDC-0720)

Related Websites

ITS_LIVE project | Overview

GoLIVE data at NSIDC | Overview

GIMP data at NSIDC | Overview

AIV data at NSIDC | Overview

How to Cite

The recommended citation is:

"*Velocity data generated using auto-RIFT (Gardner et al., 2018) and provided by the NASA MEaSUREs ITS_LIVE project (Gardner et al., 2019).*"

Gardner, A. S., M. A. Fahnestock, and T. A. Scambos, 2019 [update to time of data download]: ITS_LIVE Regional Glacier and Ice Sheet Surface Velocities. Data archived at National Snow and Ice Data Center; doi:10.5067/6II6VW8LLWJ7.

Gardner, A. S., G. Moholdt, T. Scambos, M. Fahnstock, S. Ligtenberg, M. van den Broeke, and J. Nilsson, 2018: Increased West Antarctic and unchanged East Antarctic ice discharge over the last 7 years, *Cryosphere*, 12(2): 521–547, doi:10.5194/tc-12-521-2018.

Contacts

All questions can be addressed to NSIDC User Services: nsidc@nsidc.org

References

Bolch, T., Sandberg Sørensen, L., Simonsen, S. B., Mölg, N., Machguth, H., Rastner, P., & Paul, F. (2013). Mass loss of Greenland's glaciers and ice caps 2003-2008 revealed from ICESat laser altimetry data. Geophysical Research Letters, 40(5), 875–881. https://doi.org/10.1002/grl.50270

Depoorter, M. A., Bamber, J. L., Griggs, J. A., Lenaerts, J. T. M., Ligtenberg, S. R. M., van den Broeke, M. R., & Moholdt, G. (2013). Calving fluxes and basal melt rates of Antarctic ice shelves. Nature, 502(7469), 89–92. https://doi.org/10.1038/nature12567

Gardner, A. S., Moholdt, G., Scambos, T., Fahnstock, M., Ligtenberg, S., van den Broeke, M., & Nilsson, J. (2018). Increased West Antarctic and unchanged East Antarctic ice discharge over the last 7 years. The Cryosphere, 12(2), 521–547. https://doi.org/10.5194/tc-12-521-2018

Joughin, I., Smith, B. E., Howat, I. M., Scambos, T., & Moon, T. (2010). Greenland flow variability from ice-sheet-wide velocity mapping. Journal of Glaciology, 56(197), 415–430. https://doi.org/10.3189/002214310792447734

Mouginot, J., Scheuchl, B., & Rignot, E. (2012). Mapping of Ice Motion in Antarctica Using Synthetic-Aperture Radar Data. Remote Sensing, 4(9), 2753–2767. https://doi.org/10.3390/rs4092753

Rignot, E., Mouginot, J., & Scheuchl, B. (2011). Ice Flow of the Antarctic Ice Sheet. Science, 333(6048), 1427–1430. https://doi.org/10.1126/science.1208336